Draft version July 18, 2006
Preprint typeset using LaTeX style emulateapj v. 7/15/03

INVERSE COMPTON EMISSION FROM GALACTIC SUPERNOVA REMNANTS: EFFECT OF THE INTERSTELLAR RADIATION FIELD

Troy A. Porter[1]
Santa Cruz Institute for Particle Physics, University of California, Santa Cruz, CA 95064

Igor V. Moskalenko[2]
Hansen Experimental Physics Laboratory, Stanford University, Stanford, CA 94305

and

Andrew W. Strong
Max-Planck-Institut für extraterrestrische Physik, Postfach 1312, D-85741 Garching, Germany

Draft version July 18, 2006

ABSTRACT

The evidence for particle acceleration in supernova shells comes from electrons whose synchrotron emission is observed in radio and X-rays. Recent observations by the HESS instrument reveal that supernova remnants also emit TeV γ-rays; long awaited experimental evidence that supernova remnants can accelerate cosmic rays up to the "knee" energies. Still, uncertainty exists whether these γ-rays are produced by electrons via inverse Compton scattering or by protons via π^0-decay. The multi-wavelength spectra of supernova remnants can be fitted with both mechanisms, although a preference is often given to π^0-decay due to the spectral shape at very high energies. A recent study of the interstellar radiation field indicates that its energy density, especially in the inner Galaxy, is higher than previously thought. In this paper we evaluate the effect of the interstellar radiation field on the inverse Compton emission of electrons accelerated in a supernova remnant located at different distances from the Galactic Centre. We show that contribution of optical and infra-red photons to the inverse Compton emission may exceed the contribution of cosmic microwave background and in some cases broaden the resulted γ-ray spectrum. Additionally, we show that if a supernova remnant is located close to the Galactic Centre its γ-ray spectrum will exhibit a "universal" cutoff at very high energies due to the Klein-Nishina effect and not due to the cut-off of the electron spectrum. As an example, we apply our calculations to the supernova remnants RX J1713.7-3946 and G0.9+0.1 recently observed by HESS.

Subject headings: Galaxy: general — gamma-rays: theory — radiation mechanisms: non-thermal — ISM: cosmic rays — ISM: supernova remnants — ISM: individual (RXJ1713.7-3946, G0.9+0.1)

1. INTRODUCTION

A new calculation (Porter & Strong 2005) of the Galactic interstellar radiation field (ISRF) consistent with multi-wavelength observations by DIRBE and FIRAS indicates that the energy density of the ISRF is higher, particularly in the inner Galaxy, than previously thought. This has implications for the inverse Compton (IC) scattering of electrons and positrons and other electromagnetic processes in the interstellar medium (Moskalenko & Strong 2000; Moskalenko et al. 2006). Another place where the enhanced ISRF may play a role is the IC emission off very high energy (VHE) electrons accelerated in a supernova remnant (SNR) shock.

SNRs are believed to be the primary sources of cosmic rays in the Galaxy. Observations of X-ray (Koyama et al. 1995) and γ-ray emission (Aharonian et al. 2005b, 2006) from SNR shocks reveal the presence of energetic particles, thus testifying to efficient acceleration processes. Acceleration of particles in collisionless shocks is a matter of intensive research in conjunction with the problem of cosmic ray origin (Drury 1983; Blandford & Eichler 1987; Jones & Ellison 1991). Current models include nonlinear effects (e.g., Berezhko & Völk 2006) and treat particle acceleration using hydrodynamic codes (e.g., Ellison & Cassam-Chenaï 2005). The predicted spectrum of accelerated particles has a power-law form in rigidity with index which may slightly vary around -2.0. Conventional estimates put the maximum reachable particle energy (protons) at or just below the knee energy; for the case of electrons the maximum energy is lower due to the synchrotron and IC energy losses (Ellison & Cassam-Chenaï 2005). Young SNRs may be capable of particle acceleration up to 10^{17} eV due to the effect of magnetic field amplification (Bell & Lucek 2001) around the shock and assuming Bohm diffusion and a Sedov expansion law.

The VHE γ-ray emission from shell-type SNRs has been modelled using leptonic (IC) and hadronic (π^0-decay) scenarios (e.g., Baring et al. 2005). The leptonic scenario fits the broad-band spectrum of a SNR assuming a pool of accelerated electrons scattered off the cosmic microwave background (CMB) producing VHE γ-rays while the magnetic field and electron spectrum

[1] Also Department of Physics and Astronomy, Louisiana State University, Baton Rouge, LA 70803
[2] Also Kavli Institute for Particle Astrophysics and Cosmology, Stanford University, Stanford, CA 94309

cut-off are tuned to fit the radio and X-ray data (e.g., Lazendic et al. 2004). The hadronic model fits the VHE γ-ray spectrum assuming a beam of accelerated protons hits a target, such as a nearby molecular cloud (Aharonian 2002). The latter, if definitively proven, would be the first experimental evidence of proton acceleration in SNRs. While there is no clear distinction between different models of VHE emission from SNRs, some authors tend to prefer the hadronic scenario since it fits better the observed spectral shape (Aharonian et al. 2006; Berezhko & Völk 2006). Such a preference, however, is made based on a simplified "one-zone" model which typically includes CMB photons only.

In this paper we evaluate the effect of the ISRF on the IC emission of electrons accelerated in SNRs located at different distances from the Galactic Centre (GC). As examples, we apply our calculations to the shell-type SNR RX J1713.7-3946 and composite SNR G0.9+0.1 recently observed by HESS (Aharonian et al. 2005a, 2006).

2. INTERSTELLAR RADIATION FIELD

The Galactic ISRF calculation uses a model for the distribution of stars in the Galaxy, a model for the dust distribution and properties, and a treatment of scattering, absorption, and subsequent reemission of the stellar light by the dust. A brief description of our calculation is available in Moskalenko et al. (2006); we re-iterate the main points here.

Our stellar model assumes a type classification based on that used in the SKY model of Wainscoat et al. (1992), with modifications to account for results from recent experiments such as 2MASS, SDSS, and others (e.g., Ojha 2001; Juric et al. 2005), and synthetic spectral modelling studies (e.g., Girardi et al. 2002).

Dust is modelled with a mixture of polycyclic aromatic hydrocarbons, graphite, and silicate. The dust grains are spherical and we include details of their absorption and scattering efficiencies, abundances, and size distribution in the scattering and heating calculations (Li & Draine 2001; Weingartner & Draine 2001). Stochastic and equilibrium heating of the dust grains is treated following Draine & Li (2001) and Li & Draine (2001). The dust is assumed to follow the Galactic gas distribution and metallicity gradient (Moskalenko et al. 2002; Strong et al. 2004, and references therein).

Figure 1 shows the total ISRF at the positions we will calculate the IC emission in Section 3. Information on the calculation method, spatial and spectral distribution in the Galactic plane, and a brief comparison of our calculations with previous results and the locally observed ISRF are given in Moskalenko et al. (2006); further discussion of the new ISRF is deferred to a forthcoming paper (Porter & Strong, in preparation).

3. CALCULATIONS

For an assumed isotropic ISRF and electron distribution, the IC emissivity (photons cm^{-3} s^{-1}) is given by

$$\frac{dP_\gamma}{d\epsilon_2} = c \int d\epsilon_1 \int d\gamma_e \, n_\epsilon(\epsilon_1) n_e(\gamma_e) \frac{dQ_\gamma(\gamma_e, \epsilon_1)}{d\epsilon_2}, \qquad (1)$$

where $\epsilon_2 = E_\gamma / m_e c^2$ and $\epsilon_1 = \epsilon / m_e c^2$ are the dimensionless γ-ray and target photon energy, $\gamma_e = E_e / m_e c^2$ is the electron Lorentz factor, n_ϵ and n_e are the differential target photon and electron number densities, and $dQ_\gamma / d\epsilon_2$ is given by eq.(9) in Jones (1968).

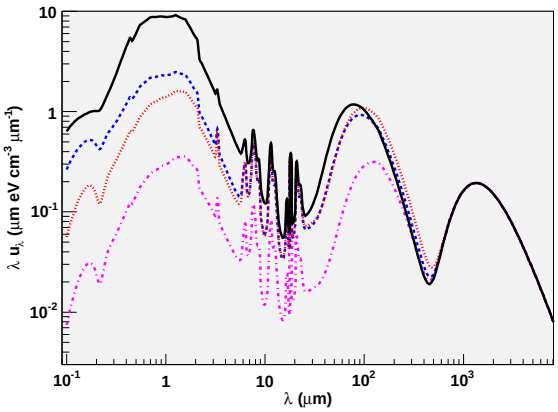

FIG. 1.— Interstellar radiation field energy density: solid line, $R = 0$ kpc, $z = 0$ kpc; dashed line, $R = 3$ kpc, $z = -0.05$ kpc; dotted line, $R = 4$ kpc, $z = 0$ kpc; dash-dotted line, $R = 7.5$ kpc, $z = 0$ kpc.

To illustrate the effect of different electron spectral indices on the IC emission, we take an electron number density $n_e(\gamma_e) = n_0 \gamma_e^{-\delta}$ normalised so that $\int_{\gamma_{\rm min}}^{\infty} n_e(\gamma_e) d\gamma_e = 1$ cm^{-3} with $\gamma_{\rm min} = 1\,{\rm MeV}/m_e c^2$ for $\delta = 1.8$, $\delta = 2.0$ and $\delta = 2.5$.

Figure 2 shows the calculated IC emissivity using the ISRF at $R = 0$ (upper) and $R = 4$ (lower) in the Galactic plane. There are two essential effects that contribute to produce the total emission curves in Fig. 2. First, the variation in the electron spectral index $\delta = 1.8 \rightarrow 2.5$ increases the contribution by optical and infra-red (IR) photons to the γ-ray emission below ~ 50 GeV and ~ 1 TeV, respectively. As δ increases, the number of low energy electrons increases; the IC scattering rate by these electrons off optical and IR photons becomes larger giving more upscattered photons. In turn, as the γ-ray energy increases, the contribution by the optical and IR photons to the total emissivity decreases from the reduction of the scattering cross-section in the Klein-Nishina (KN) regime. Thus, softer electron spectra promote more efficient scattering of the optical and IR components, increasing their relative contributions. Second, the density of optical and IR photons varies with position in the Galaxy. Toward the GC, the optical photon density is high, almost an order of magnitude larger per target photon energy interval when compared with the optical component at $R = 4$ kpc. Similarly, over the inner Galaxy the IR photon energy density is significantly higher than the CMB. This gives a contribution by the optical and IR photons to the total IC emission that is at least comparable to the CMB over these regions of the Galaxy.

Note that the marked decrease in the optical, then IR, then CMB emission as the γ-ray energy increases in Fig. 2 is due to the reduction of the scattering cross-section in the KN regime, as described above, and not due to any cut-off we have introduced in the electron spectrum; if a cut-off was included in the electron spectrum, it would further decrease the contribution from the CMB relative to the optical and IR components (see Fig. 4).

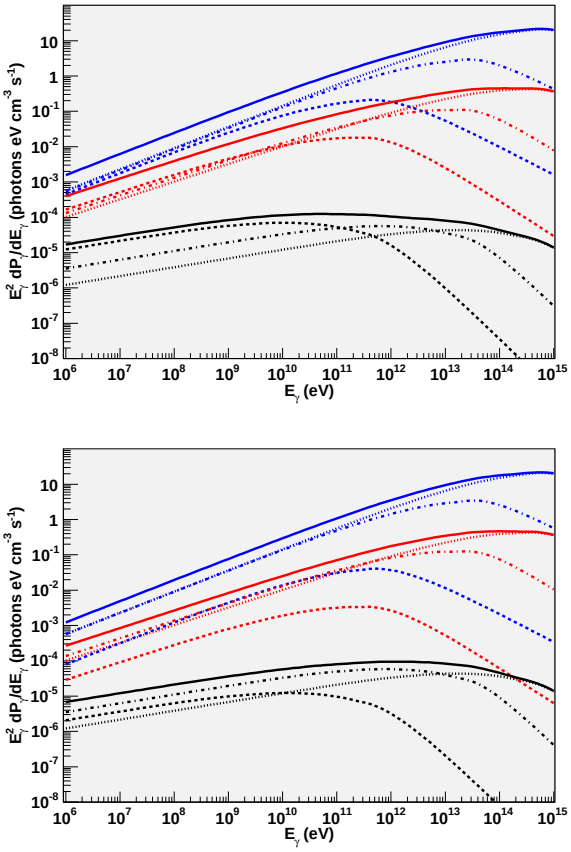

FIG. 2.— Inverse Compton emissivity in the Galactic plane for $R = 0$ kpc (top) and $R = 4$ kpc (bottom). Line styles: solid line, total; dashed, optical; dot-dashed, infra-red; dotted, CMB. For each panel, top-most line-sets correspond to $\gamma_e^{-1.8}$, middle line-sets correspond to $\gamma_e^{-2.0}$ and bottom-most correspond to $\gamma_e^{-2.5}$ electron spectra respectively.

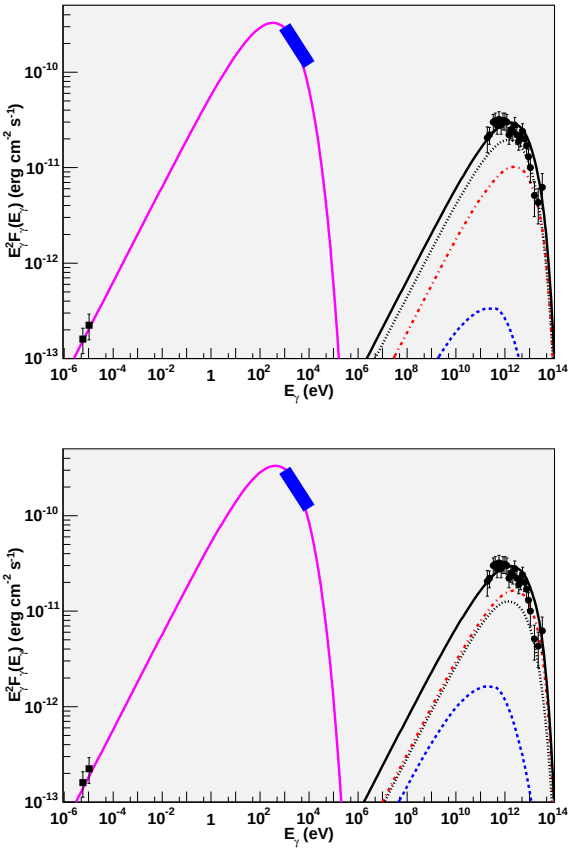

FIG. 3.— Fit to the flux spectrum of RXJ1713.7-3946 using the ISRF for $d = 1$ kpc (upper) and $d = 6$ kpc (lower). Line-styles: solid, total synchrotron and IC flux; dashed, optical IC; dash-dotted, infra-red IC; dotted, CMB IC. Data: radio (ATCA) from Lazendic et al. (2004) for the north-west rim of RXJ1713.7-3946, but upscaled by a factor of 2 following Aharonian et al. (2006); X-ray (ASCA) from Pannuti et al. (2003); γ-ray (HESS) from Aharonian et al. (2006).

To illustrate the effect of the ISRF in a purely leptonic scenario, we calculate the synchrotron and IC emission using a one-zone model (Aharonian & Atoyan 1999) for the SNR RXJ1713.7-3946. We use an electron spectrum $Q_e(E) = Q_0 E^{-\delta} \exp(-E/E_{\rm max})$ where Q_0, δ and $E_{\rm max}$ are adjustable parameters. The synchrotron emission for a magnetic field strength B is calculated using the usual formulae (Ginzburg 1979; Ghisellini et al. 1988).

Figure 3 shows the photon flux from RXJ1713.7-3946 calculated for a distance of $d = 1$ kpc (upper) and $d = 6$ kpc (lower). This covers the range of distances quoted by various authors (Lazendic et al. 2004; Aharonian et al. 2006). The IC emission is calculated using the appropriate ISRF spectrum for each distance (see Fig. 1). For both cases, we reproduce the TeV emission first: with $\delta \sim 1.8 - 2.2$ and $E_{\rm max} \sim 15 - 40$ TeV a reasonable fit can be obtained. Next, we fit the radio and X-ray data within the constraints imposed by the TeV emission: $\delta \sim 2.0$ and $E_{\rm max} \sim 15 - 25$ TeV, with $B \sim 5 - 20$ μG are allowed. The electron luminosity for an age of 1000 years ($d = 1$ kpc) or 10000 years ($d = 6$ kpc) is $(1-4)\times10^{37}$ erg s^{-1} with larger luminosities for the more distant case. The parameters used are not unique. As a particular example, the values used in Fig. 3 are: $\delta = 2.0$, electron luminosity of 1.5×10^{37} erg s^{-1}, $E_{\rm max} = 25$ TeV, and $B = 12$ μG ($d = 1$ kpc); $\delta = 2.0$, electron luminosity of 3.5×10^{37} erg s^{-1}, $E_{\rm max} = 25$ TeV, and $B = 15$ μG ($d = 6$ kpc).

We also consider the composite SNR G0.9+0.1 observed by HESS (Aharonian et al. 2005b); this composite SNR is a source of VHE electrons, as evidenced by the synchrotron X-ray emission (Porquet et al. 2003), and is located in the GC region where the ISRF density is high. As for RXJ1713.7-3946, we use a one-zone model except we modify the source spectrum to be a broken power-law with a break at energy $E_{\rm break}$. As before, we adjust the electron luminosity and high energy spectral index to fit the TeV observations, then vary B and $E_{\rm max}$ to reproduce the X-ray data. Then, $E_{\rm break}$ and the low energy spectral index are adjusted to give consistency with the radio data. Figure 4 shows the calculated intrinsic photon flux for G0.9+0.1 at the GC. The parameter values are: $\delta_L = 2.0$, $\delta_U = 2.8$, $E_{\rm break} = 15$ GeV, where δ_L and δ_U are the spectral indices below and above $E_{\rm break}$ respectively, $B = 9.5$ μG, $E_{\rm max} = 1000$ TeV, and an electron luminosity 2.5×10^{38} erg s^{-1} for an assumed age of 5000 years. Note that these values are again not unique, and other combinations are possible.

The cut-off in the IC emission for the optical and IR

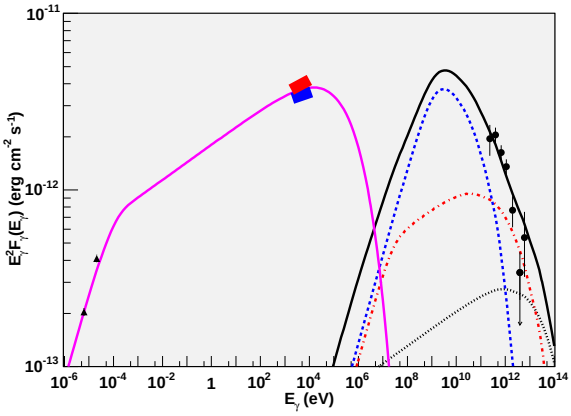

FIG. 4.— Fit to the flux spectrum of G0.9+0.1. Line-styles as for Fig. 3. Data: radio (VLA) from Helfand & Becker (1987); X-ray (BeppoSAX) at 1.8–10 keV from Sidoli et al. (2000) (upper solid region) and (XMM) at 2–12 keV from Porquet et al. (2003) (lower solid region); γ-ray (HESS) from Aharonian et al. (2005a).

in Figs. 3 and 4 comes from the reduction of the scattering cross-section in the KN regime; only for the CMB is the IC spectral cut-off solely due to the cut-off in the electron spectrum. The cut-off in the IC emission for the IR in Fig. 3 is only partially due to the KN effect since the electron spectral cut-off energy is essentially lower. This effect plays an important role for a SNR close to the GC where the ISRF is dominant. In this case, the cut-off energy of the VHE γ-ray spectrum becomes universal and defined exclusively by the reduction of the scattering cross-section and not by an assumed electron spectral cut-off. Note also, for energies higher than ~ 10 TeV, the intrinsic spectrum will be further reduced by attenuation due to pair production on the ISRF itself (Moskalenko et al. 2006).

4. DISCUSSION

We have evaluated the effect of the ISRF on the IC emission of electrons accelerated in SNRs. Our calculation shows that for a SNR located in the inner Galaxy the contribution of optical and IR photons to the IC emission exceeds the contribution of the CMB and in some cases broadens the resultant γ-ray spectrum. SNRs located close to the GC exhibit a "universal" cut-off at VHEs due to the KN effect and not due to a cut-off in the electron spectrum.

We have made a calculation of the IC and synchrotron emission for simple power-law electron spectra including the contribution by the ISRF using the shell-type SNR RXJ1713.7-3946 and composite SNR G0.9+0.1 as examples. Within the confines of a simple one-zone leptonic model, it is possible to fit the observed flux spectrum with a reasonable combination of model parameters. Observations in the GeV to sub-TeV range by the GLAST experiment will be critical in distinguishing between leptonic or hadronic scenarios of γ-ray production in SNRs as the predictions for the spectral shape in this energy range are distinctly different.

Finally, we point out at least two cases for the leptonic model where the contribution of the ISRF will be critical. First will be when fitting the synchrotron peak dictates a relatively *low-energy* cut-off in the electron spectrum. In this case, the VHE γ-rays will be produced by lower-energy electrons scattered off optical and IR photons. Second will be when fitting the synchrotron peak dictates a *high-energy* cut-off in the electron spectrum. An equal or exceeding contribution of optical and IR protons, but with lower energy cut-off in the spectrum of upscattered γ-rays due to the KN effect, will effectively broaden the IC peak. Observations of the TeV emission from SNRs in the inner Galaxy may thus serve as a probe of the ISRF near their location. In turn, observations of shell-type SNRs in the outer Galaxy where the CMB photons will provide the majority of the IC emission may be used to evaluate the spectrum of accelerated electrons in the shell and for studies of shock acceleration.

We thank Olaf Reimer for useful discussions. T. A. P. acknowledges partial support from the US Department of Energy. I. V. M. acknowledges partial support from NASA Astronomy and Physics Research and Analysis Program (APRA) grant.

REFERENCES

Aharonian, F. & Atoyan, A. M., 1999, A&A, 351, 330
Aharonian, F., 2002, Nature, 416, 797
Aharonian, F., et al., 2005a, A&A, 432, L25
Aharonian, F., et al., 2005b, A&A, 437, L7
Aharonian, F., et al., 2006, A&A, 449, 223
Baring, M. G., Ellison, D. C., & Slane, P. O., 2005, Adv. Sp. Res., 35, 1041
Bell, A. R. & Lucek, S. G., 2001, MNRAS, 321, 433
Berezhko, E. G. & Völk, H. J., 2006, A&A, 451, 981
Blandford, R. & Eichler, D., 1987, Phys. Rep., 154, 18
Draine, B. T. & Li, A., 2001, ApJ, 551, 807
Drury, L., 1983, Sp. Sci. Rev., 36, 57
Ellison, D. C. & Cassam-Chenaï, G., 2005, ApJ, 632, 920
Ghisellini, G., Guilbert, P. W., & Svensson, R., 1988, ApJ, 334, L5
Ginzburg, V. L., "Theoretical physics and astrophysics", International Series in Natural Philosophy (Oxford: Pergamon) (1979)
Girardi, L., et al., 2002, A&A, 391, 195
Helfand, D. J. & Becker, R. H., 1987, ApJ, 314, 203
Henyey, L. G. & Greenstein, J. L., 1941, ApJ, 93, 70
Jones, F. C., 1968, Phys. Rev., 167, 1159
Jones, F. C. & Ellison, D. C., 1991, Sp. Sci. Rev., 58, 259
Juric, M., et al., ApJ submitted, 2005, arXiv : (astro-ph/0510520)
Koyama, K., et al., 1995, Nature, 378, 255
Lazendic, J. S., et al., 2004, ApJ, 602, 271
Li, A. & Draine, B. T., 2001, ApJ, 554, 778
Mereghetti, et al., 1998, A&A, 331, L77
Moskalenko, I. V. & Strong, A. W., 2000, ApJ, 528, 357
Moskalenko, I. V., Strong, A. W., Ormes, J. F., & Potgeiter, M. S., 2002, ApJ, 565, 280
Moskalenko, I. V., Porter, T. A., & Strong, A. W., 2006, ApJ, 640, L155
Ojha, D. K., 2001, MNRAS, 322, 426
Pannuti, T. G., et al. 2003, ApJ, 593, 377
Porquet, D., et al., 2003, A&A, 401, 197
Porter, T. A. & Strong, A. W., 2005, in Proc. 29$^{\rm th}$ Int. Cosmic Ray Conf. (Pune) (astro-ph/0507119)
Sidoli, L., et al., 2000, A&A, 361, 719
Strong, A. W., Moskalenko, I. V., Reimer, O., Digel, S. & Diehl, R., 2004, A&A, 422, L47
Wainscoat, R. J., et al., 1992, ApJS, 83, 111
Weingartner, J. C. & Draine, B. T., 2001, ApJ, 548, 296